Int. J. Electrochem. Sci., 16 **(2021)** Article ID: 210642, doi: 10.20964/2021.06.15

International Journal of ELECTROCHEMICAL SCIENCE
www.electrochemsci.org

Short Communication

Electrochemical Evaluation on Corrosion Behavior of SAF 2507 Duplex Stainless Steels in Blended Concrete with Metakaolin and ultrafine Slag Admixtures

Taoli Xiao[1,*], *Chenchen Du*[2], *Yongle Liu*[3]

School of Urban Construction, Yangtze University, Jingzhou 434023, Hubei, China
[*]E-mail: 200536@yangtzeu.edu.cn

Received: 30 June 2020 / *Accepted:* 16 August 2020 / *Published:* 30 April 2021

The supplementary cementitious materials can be used in the construction industry as a replacement of Portland cement (PC) to minimize the corrosion of steel rebar. In this work the effect of ultrafine slag (US) and metakaolin as partial replacement of PC on strength concrete and electrochemical corrosion behavior of SAF2507 duplex stainless steel (DSS) rebars were studied. The DSS reinforced concrete specimens were exposed to 3.5wt% NaCl solution. The mechanical results for concrete specimens indicated a considerable increase in compressive strength in the PC blended with both metakaolin and US (15M15US).The electrochemical results indicated that the 15M15US sample had higher value of corrosion resistance than the other samples. The surface morphologies of DSS rebars indicated that narrow pits and low production of corrosion were observed on the 15M15US sample which was in agreement with the results attained from electrochemical tests.

Keywords: Electrochemical corrosion; Supplementary cementitious materials; Duplex stainless steels; Mechanical properties

1. INTRODUCTION

Stainless steel rebar is an efficient technique for corrosion protection of reinforced concrete structures [1]. Austenitic and ferritic stainless steels were the first developed stainless steel rebars, the current trend is to use duplex stainless steel (DSS)[2]. The stainless steel passivates in the atmosphere area[3]. However, the passive layer is not stable when the DSS comes into contact with the alkaline media of concrete and a new process of passivation takes place [4]. DSS, as a kind of structural materials, are widely used in chemical, petrochemical, marine, nuclear and paper industries due to their excellent combination of mechanical properties and corrosion resistance in various types of environments. Given that the SAF 2507 is one of the most widely used DSS grades, in this study we used this type of DSS as a rebar. Numerous researches with SS reported their suitable corrosion resistance in environments contained with chloride ions [5, 6]. The chemical admixtures including mixing water, chlorides, and use of polluted aggregates can lead to the internal availability of chloride ions in the concrete structure [7]. These chloride ions are more destructive rather than the external chloride ions when these chlorides are seen in the interface of concrete-steel even before the formation of thin passive film which essentially forms during the cement hydration process[8].

Many research had been done to reduce the cost of repairs and increase the durability of reinforced rebars, particularly those exposed to marine media[9].Several researchers had been using admixtures into concrete structures to develop their delay and durability in the corrosion[10]. The typical admixtures are silica fume, calcium nitrite, blast furnace slag, fly ash, hydroxyl alkylamines, metakaolin and sodium monofluorophosphate[11, 12]. The logic behind using these materials is simple. They form a denser concrete, decrease its permeability, limit ion flow, and enhance electrical resistance and slow corrosion current. Many researchers had revealed that supplementary cementitious materials (SCMs) reduced chloride penetration and porosity[13]. Incorporating SCMs into a concrete mix decreases the capillary pores of concrete and reduces its penetrating properties[14]. As a result, it becomes more difficult to achieve surface of steel reinforcement for chloride-contaminated water.

Replacement of fine aggregates may cause enhanced stability using pore refinement and improved resistance to the release of harmful agents[15]. Many studies had shown that the mineral admixtures strangely increased the resistance to diffusion of chloride in SCM. However, the simultaneous effects of metakaolin and ultrafine slag on the corrosion behavior of DSS reinforced concrete had not been previously reported. In this work, a study on corrosion resistance of DSS rebar in concrete with partial replacement of cement by metakaolin and ultrafine slag was done. The electrochemical method was used to investigate corrosion properties of the specimens in 3.5 wt% NaCl solution as marine environment.

2. MATERIALS AND METHOD

In order to investigate the mechanical and electrochemical properties of concrete samples replacement with metakaolin and ultrafine slag, compressive strength and electrochemical tests were done on the samples. In this work, the different components of cement for production of reinforced concrete which contained different mixture proportions of Portland cement (PC), metakaolin and ultrafine slag (US) were used. Table 1 exhibits the chemical properties of cement admixtures.

Table 1. Chemical property of PC, metakaolin and US

	PC (wt%)	Metakaolin (wt%)	US(wt%)
SiO_2	20.55	51.71	36.41
Al_2O_3	4.84	42.98	10.39
Fe_2O_3	3.12	0.96	0.69
CaO	64.15	0.24	34.12
MgO	2.02	0.17	10.26
K_2O	0.67	0.15	0.97
Na_2O	0.23	0.01	0.35
SO_3	2.99	0.00	0.00
LOI	0.89	0.56	1.64

Table 2 shows the proportions of mixes for every samples. The PC was blended with sand, gravel, and water (1.5: 3: 1: 0.5) to produce concrete structure. The prepared mixtures were poured in the cylindrical molds with a radius of 5 cm and a height of 15 cm. Then the samples were kept at 25 ^{o}C temperature for 24 hours.

Table 2. The proportions of mixes for different concrete structures

Sample	PC (wt%)	Metakaolin (wt%)	US (wt%)
PC	100	0	0
30M	70	30	0
30US	70	0	30
15M15US	70	15	15

In order to study the effect of metakaolin and US admixtures on corrosion resistance of the DSS rebar, electrochemical tests were performed on SAF2507DSS rebar. In order to prepare working electrode, the concrete mixture was poured into the cylindrical mold, while a steel rebar was placed vertically at the center of the cylinder. The DSS rebar had 10 mm diameter and 150 mm length. Table 3 indicates the composition of the SAF2507 duplex stainless steel rebar.

Table 3. Composition of SAF2507 duplex stainless steel rebar (wt%)

C	Mn	Si	P	S	N	Mo	Cr	Ni	Fe
0.025	1.25	0.80	0.035	0.020	0.25	3.18	25.54	5.0	Residual

A three-electrode electrochemical system was applied to consider the electrochemical corrosion properties of the specimens. Steel reinforced concrete, a standard copper/copper sulfate electrode and graphite were utilized as the working, reference and counter electrodes. The samples immersed into the 3.5 wt% NaCl solution as a marine environment. The obtained results were analyzed by using specialized software. Electrochemical impedance spectroscopy (EIS) analyses were done in the frequency range of 100 kHz to 0.1 mHz. The cyclic voltammetry analysis was carried out between -1.2V and 0.8 V at scan rate with 50 mV/s. The polarization test was performed from 0.25V at scanning rate of 1 mV/s. The compressive strength experiments were done for three specimens for every mixtures for 2 days, 1 week, 2 weeks and 4 weeks according to IS 516e1959 specification. A scanning electron microscope (SEM) was used to investigate the surface morphologies ofSAF2507 DSS rebars.

3. RESULTS AND DISCUSSION

The compressive strength of the samples are shown in figure 1. By comparing the different replacement mixtures, it can be concluded that at any age the 15M15US sample has a higher strength. The increase in strength can be due to the high concentration of CaO in US. It reacts both in hydraulic and pozzolanic manner which results in high strength denser and pore structure. It was also concluded that 15M15US mixtures show high strength compared to other samples. Furthermore, concrete with the US showed a higher initial strength at each percentage US replacement. The final strength was also higher than the PC concrete.

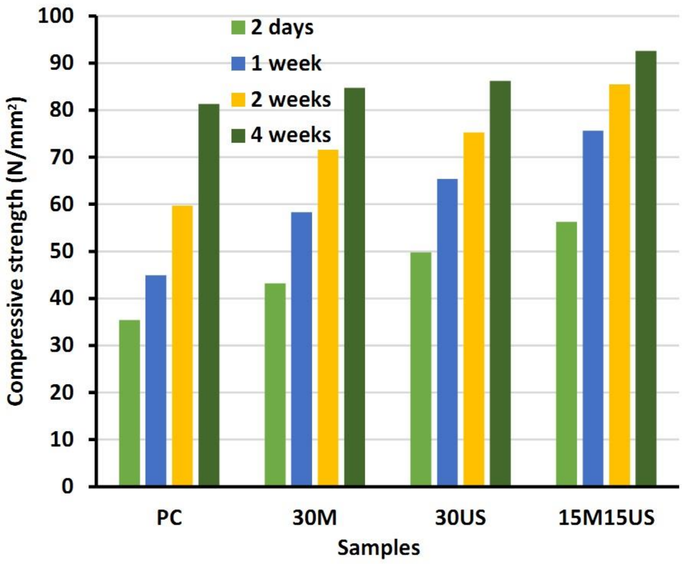

Figure 1. Compressive strength of the samples with different replacement mixtures at room temperature

Figure 2 shows polarization plots of DSS rebar in different concrete specimens exposed to 3.5 wt% NaCl solution after 4 weeks exposure time. As indicated in figure 2, the anodic polarization plots were studied by passive zones at DSS rebars, revealing the passive films had obviously formed on the DSS surface when they were exposed to 3.5 wt% NaCl solution. Furthermore, a considerable shift was found in corrosion potential toward a positive direction, which indicated that with the change in the concrete admixtures, the dissolution of anode steel was effectively delayed.

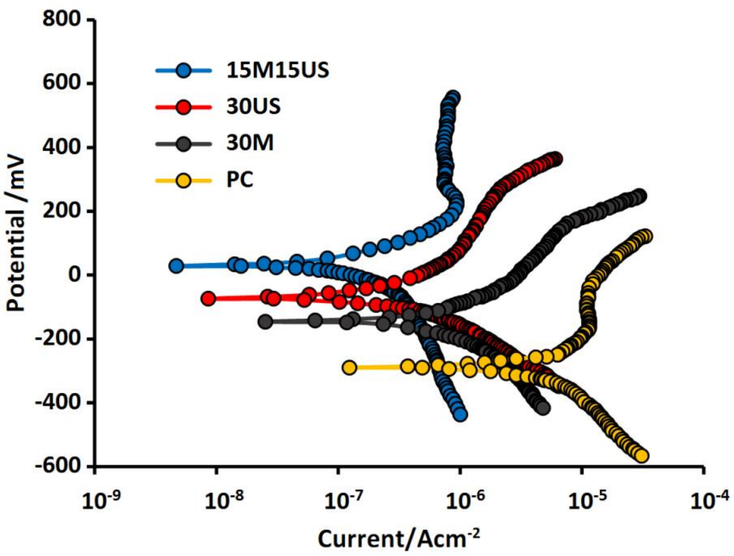

Figure 2. Potentiodynamic polarization of DSS rebar embedded in various concrete specimens exposed to 3.5 wt% NaCl solution after 4 weeks exposure time at scanning rate of 1 mV/s.

Table 4. Corrosion potential, corrosion current density, cathodic Tafel slope and corrosion rate of DSS rebar embedded in various concrete specimens

Mixtures	Corrosion current density ($\mu A/cm^2$)	Corrosion potential (mV)	β_c ($mVdec^{-1}$)	R_p($k\Omega\ cm^2$)
PC	3.52	-286	159	9.25
30M	0.71	-148 V	148	42.31
30US	0.63	-116 V	129	49.86
15M15US	0.48	44 V	81	387.58

Compared to all the specimens, the passive area in the 15M15US sample was much wider. Furthermore, the passive current density of DSS rebar embedded in concrete sample replaced with both Metakaolin and US was lower than other samples, indicating the corrosion protection of passivated DSS was enhanced for 15M15US specimen. More corrosion resistance in 15M15US sample can be related to the Metakaolin and US that had reacted with the released calcium hydroxide ($Ca(OH)_2$) at the hydration of cement and formed extra calcium silicate hydrate, which enhanced the durability and mechanical properties of the concrete samples [23]. The values of corrosion potential (E_{corr}) and corrosion current density (I_{corr}) are shown in table 4, which is attained from the polarization curves in Figure 2. The permeability of concrete is directly related to the concrete content. On the other hand, lower permeability leads to the production of denser concrete [16]. This means that fewer ions were allowed to enter the concrete samples. Therefore, the I_{corr} will be less and the E_{corr} will be more positive. The lower current density in the 15M15US sample can be attributed to the change in the structure or the thickness of the passive layer on the steel rebars [28].

The corrosion level can be defined at 4-levels introduced by Durar Network Specification [17]. However, the I_{corr} of 15M15US specimen into3.5 wt% NaCl solution was lower than other samples (Table 4). Therefore, the DSS reinforced concretes in 15M15US sample stayed into the passive state during test process which indicated its excellent corrosion resistance of DSS rebar in the 3.5 wt% NaCl solution [18].

Furthermore, cathodic Tafel slope (β_c) was measured from the Tafel extrapolation technique. As revealed in table 4, β_c value changes in different concrete specimens. The change in the Tafel slope value can be utilized to classify the inhibition mechanism for DSS, charge transfer coefficient, composition of working electrode and concentration of electrolyte[19].The values of the β_c, significantly changed in different concrete specimens, which suggested that its effect on the cathodic reaction modified the hydrogen evolution discharge mechanism[20]. Moreover, the Tafel slope reduced in 15M15US sample, which meant metakaolin and US combination in concrete could help the corrosion resistance of DSS rebars in 3.5 wt% NaCl solution.

Since electron conductive paths may be formed by adding US, thus the current density and the electrical resistivity of the DSS rebar had reduced. Moreover, the side effects of US on corrosion resistance of DSS reinforced concrete maybe offset by addition of metakaolin, which had no significant effect on resistivity of US concrete but can reduce the porosity and water absorptivity. Furthermore, metakaolin can optimize the US dispersion in concrete structure. Thus, the addition of metakaolin and

US simultaneously assists to improve concrete structure which decreases the absorption of chloride ions and water on the DSS rebar.

The value of corrosion current density in this work was comparable with other obtained values for SS rebars from the other researchers [21-24]. The i_{corr} reached during passivation of the DSS rebars in concrete depended on the SS grade used, as Bertolini and Gastaldi also proposed in [25]. These differences in the passivation i_{corr} were related to different composition of the passive films because of differences in concrete-rebar interface, as a result of the chemical composition of the pore alkaline environment, and to the DSS composition, as proposed also by other authors [26-28]. Different electrical conductivity because of the types of oxides predominating in the passive film were detected. Changes in the passive film composition with the various grades of DSS reinforcement used, and differences in the pore alkaline composition produced during the hydration of the different binders were responsible for the different i_{corr} at the passive state.

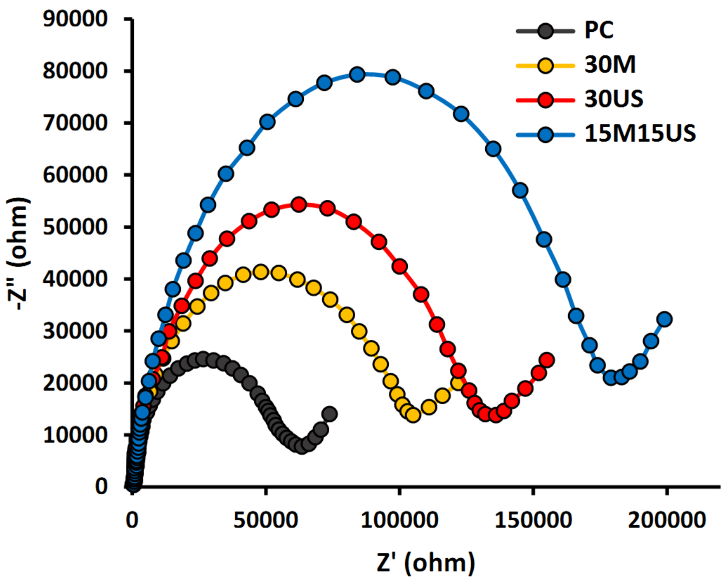

Figure 3. EIS plots attained from DSS reinforced concretes produced with various admixtures at 3.5 wt% NaCl solution in the frequency range of 100 kHz to 0.1 mHz at room temperature.

EIS technique was used to consider the corrosion resistance of DSS reinforced concretes produced with various admixtures at 3.5 wt% NaCl solution. The Nyquist plots obtained from EIS analysis is shown in Figure 3. Figure 4 reveals an equivalent circuit model used in this study where R_s is solution resistance. R_f and C_f indicate the resistance and the capacitance of coated concrete, respectively [29]. C_{dl} and R_{ct} are the double-layer capacitance and the charge transfer resistance of the carbon steel surface, respectively [30]. The obtained data are shown in Table 5.

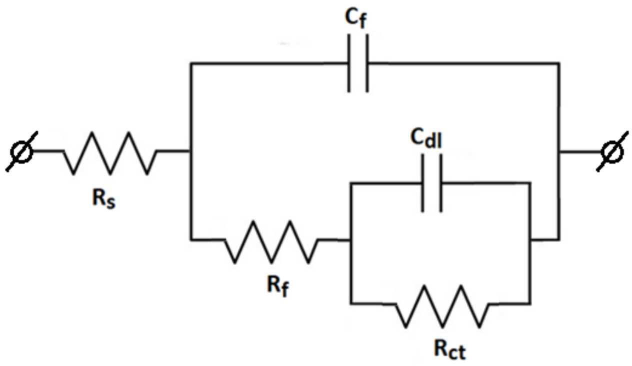

Figure 4. An equivalent circuit model used

Table 5. The obtained data for DSS reinforced concrete produced with various admixtures at 3.5 wt% NaCl solution.

Mixtures	R_s (Ω)	R_f (kΩ)	C_f(µF cm^{-2})	R_{ct} (kΩ)	C_{dl}(µF cm^{-2})
PC	26.4	48.24	10.2	62.53	13.8
30M	28.5	78.92	6.3	111.36	8.6
30US	31.2	96.58	4.8	138.62	7.3
15M15US	29.7	14.66	4.1	191.07	5.4

The thickness of the passive layer can be measured with the following equation [31]:

$$D = \frac{\varepsilon\varepsilon_0 A}{C_{dl}} \qquad (1)$$

Where D is the passive film thickness, ε_0 (8.85×10^{-12} F m^{-1}) and ε (12 for Fe oxides) are the vacuum permittivity and dielectric constant, respectively. A is an effective area and capacitance.

As indicated in table 5, the value of C_{dl} decreases in PC concrete containing admixtures, which reveals that the passive film thickness was increased and the resulting protective capacity was enhanced when the metakaolin and US was replaced in the PC cement.

As indicated in table 5, with the proper replacement of metakaolin and US in the PC cement, R_f increases and C_f decreases, which shows an improvement in the corrosion resistance, stability and thickness of the passive film on the DSS rebar [32]. The metakaolin has a pozzolanic reaction by the calcium hydroxide ($Ca(OH)_2$) crystals and form a dense, insoluble and monolithic gel of $Ca(OH)_2$ [33]. In addition, the SU can make a strong adhesion to hydrated cement due to the high surface area that causes a superior inhibition of the $Ca(OH)_2$ growth. These admixtures filled up the tiny cracks and capillary pores and then shrunk the structure of cement. These factors enhance the corrosion resistance of DSS rebars in aggressive media. Moreover, comparing C_{dl} and C_f, it was observed that C_f was lower than C_{dl} in all specimens which confirm the creation of thin passive layer.

In order to investigate the passive layer formation and redox reactions on the specimens in the aggressive environment, CV analyses was used. Figure 5 indicates the cyclic voltammograms of specimens in 3.5 wt% NaCl solution. The cathodic and anodic peak potentials can be found in Fig.5.

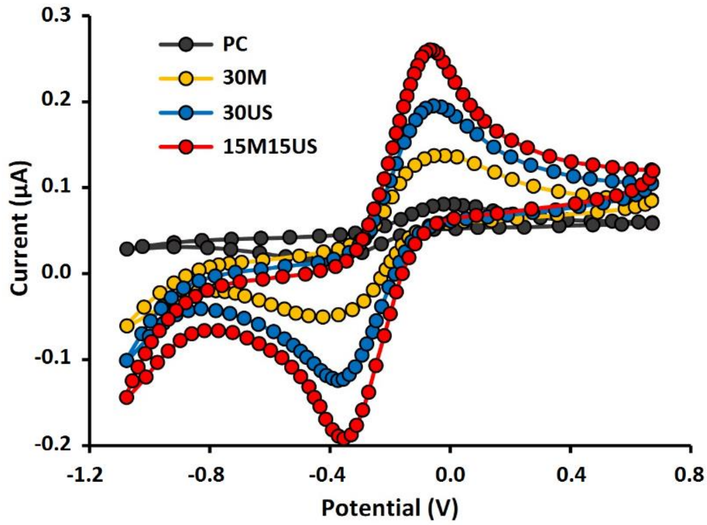

Figure 5. Cyclic voltammograms of the DSS reinforced concretes produced with various admixtures at 3.5 wt% NaCl solution at scan rate with 50 mV/s at room temperature

The anodic peak appeared at an approximate potential of -0.18 V for all specimens that was associated to transformation from Fe^{2+}ions to Fe^{3+} ions and formation of passive film on the surface of DSS rebars [34].

The current density value in zero potential (i_0) may reveal the corrosion resistance of passive film[35]. A higher value suggests weaker corrosion resistance. As indicated in figure 5, 15M15US sample shows lower i_0, revealing lower corrosion. The decrease in i_0 can be related to the stability of the passive films formed on the DSS surface. As revealed in figure 5, the cathodic peak observed at the potential of -0.38 V. Once the potential had moved to more negative values, the cathodic current density rapidly increased which can be attributed to the electrochemical procedure controlled by hydrogen development.

A significant change in the performance of DSS reinforced concrete was observed due to the use of various fillers and mineral admixtures as a partial replacement and it was more clear when both metakaolin and US admixtures was used.

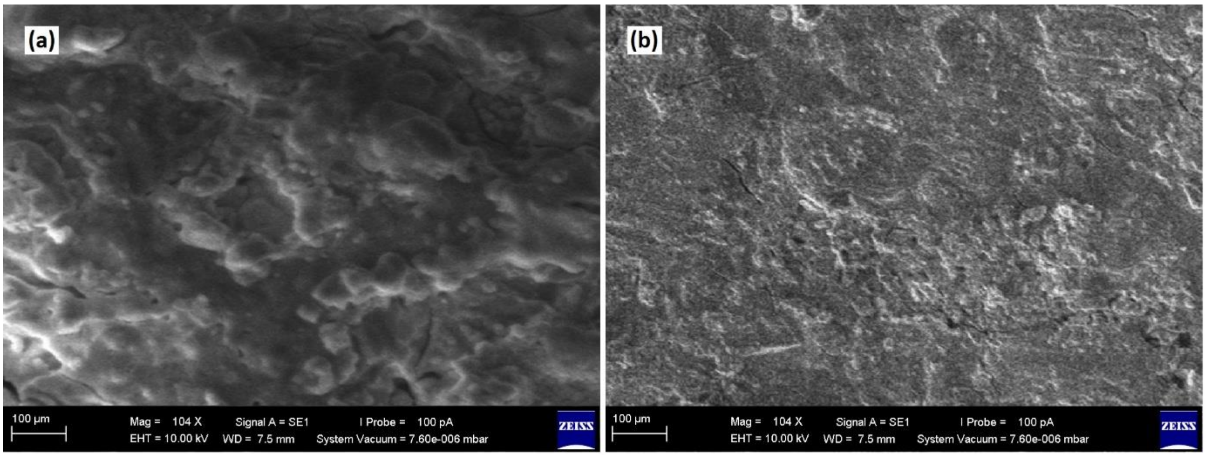

Figure 6. SEM images of DSS rebar embedded in (a) PC and (b) 15M15US concretes exposed to 3.5 wt% NaCl solution after 4 weeks exposure time at room temperature

Figure 5 indicates the SEM images of DSS rebar embedded in PC and 15M15US concretes exposed to 3.5 wt% NaCl solution after 4 weeks exposure time. Corrosion pitting on the DSS surface embedded into 15M15US concrete was considerably lower than that of DSS rebar embedded into PC concrete, indicating that the 15M15US samples were showing a superior corrosion resistance.

4. CONCLUSIONS

In this work the effect of US and metakaolin as partial replacement of PC on strength concrete and electrochemical corrosion behavior of SAF2507 DSS rebars were studied. The DSS reinforced concrete specimens were exposed into 3.5 wt% NaCl solution. The mechanical results for concrete specimens indicated a considerable increase in compressive strength in the 15M15US. The EIS results indicated that the C_{dl} value reduced for the specimen containing both US and metakaolin, showing the passive layer thickness had increased which lead to an enhanced protective capacity. The electrochemical results indicated that the 15M15US sample had higher value of corrosion resistance than the other samples. The surface morphologies of DSS rebars indicated that narrow pits and low production of corrosion were observed on the 15M15US sample which was in agreement with the results attained from electrochemical tests.

ACKNOWLEDGEMENTS
This work was supported by the Natural Science Foundation of China (grant number: 51678066), Jingzhou science and technology plan project, Hubei province (grant number: 2019CC48, 2019AC27)

References

1. M.C. Alonso, F. Luna and M. Criado, *Construction and Building Materials,* 199 (2019) 385.

2. U. Martin, J. Ress, J. Bosch and D. Bastidas, *Electrochimica Acta*, 335 (2020) 135565.
3. Y. Zhao, D.-y. Zhang, J.-j. Guan, F. Liu, P. Liang, C.-q. Cheng and J. Zhao, *International Journal of Electrochemical Science*, 14 (2019) 301.
4. H.A. Ariza-Figueroa, J. Bosch, M.A. Baltazar-Zamora, R. Croche, G. Santiago-Hurtado, L. Landa-Ruiz, J.M. Mendoza-Rangel, J.M. Bastidas, F. Almeraya-Calderón and D.M. Bastidas, *Materials*, 13 (2020) 2412.
5. H. Luo, H. Su, C. Dong and X. Li, *Applied Surface Science*, 400 (2017) 38.
6. Y. Song, G. Jiang, Y. Chen, P. Zhao and Y. Tian, *Scientific reports*, 7 (2017) 1.
7. Y. Abbas, F. Pargar, D.A. Koleva, K. van Breugel, W. Olthuis and A. van den Berg, *Construction and Building Materials*, 174 (2018) 376.
8. H. Gerengi, Y. Kocak, A. Jazdzewska and M. Kurtay, *Comput Concrete*, 19 (2017) 161.
9. R.E. Melchers, *Journal of Marine Science and Engineering*, 8 (2020) 290.
10. H. Lopez-Calvo, P. Montes-Garcia, E. Alonso-Guzmán, W. Martinez-Molina, T. Bremner and M. Thomas, *Canadian Journal of Civil Engineering*, 44 (2017) 918.
11. G. Li, A. Zhang, Z. Song, S. Liu and J. Zhang, *Construction and Building Materials*, 158 (2018) 640.
12. N. Chousidis, I. Ioannou, E. Rakanta, C. Koutsodontis and G. Batis, *Construction and Building Materials*, 126 (2016) 86.
13. S. Cheng, Z. Shui, T. Sun, R. Yu and G. Zhang, *Construction and Building Materials*, 171 (2018) 44.
14. K.M. Rahla, R. Mateus and L. Bragança, *Journal of Cleaner Production*, 220 (2019) 445.
15. H. Guo, C. Shi, X. Guan, J. Zhu, Y. Ding, T.-C. Ling, H. Zhang and Y. Wang, *Cement and Concrete Composites*, 89 (2018) 251.
16. K. Tan and J. Zhu, *Materials and Structures*, 50 (2017) 56.
17. W. Zhao, J. Zhao, S. Zhang and J. Yang, *International Journal of Electrochemical Science*14 (2019) 8039.
18. A.T. Yousefi, S. Ikeda, M.R. Mahmood, J. Rouhi and H.T. Yousefi, *World Applied Sciences Journal*, 17 (2012) 524.
19. Y. Zhou, S. Xu, L. Guo, S. Zhang, H. Lu, Y. Gong and F. Gao, *RSC Advances*, 5 (2015) 14804.
20. A. Ansari, M. Znini, I. Hamdani, L. Majidi, A. Bouyanzer and B. Hammouti, *Journal of Materials and Environmental Science*, 5 (2014) 81.
21. F. Lollini, M. Carsana, M. Gastaldi and E. Redaelli, *Corrosion Reviews*, 37 (2019) 3.
22. W. Nguyen, J.F. Duncan, T.M. Devine and C.P. Ostertag, *Electrochimica Acta*, 271 (2018) 319.
23. A. Bautista, E. Paredes, S. Alvarez and F. Velasco, *Corrosion Science*, 102 (2016) 363.
24. I.G. Ogunsanya and C. Hansson, *Corrosion*, 76 (2020) 114.
25. L. Bertolini and M. Gastaldi, *Materials and Corrosion*, 62 (2011) 120.
26. C. Abreu, M. Cristóbal, R. Losada, X. Nóvoa, G. Pena and M. Pérez, *Electrochimica Acta*, 49 (2004) 3049.
27. D. Addari, B. Elsener and A. Rossi, *Electrochimica Acta*, 53 (2008) 8078.
28. B. Elsener, D. Addari, S. Coray and A. Rossi, *Materials and Corrosion*, 62 (2011) 111.
29. K.M. Emran and H. AL-Refai, *International Journal of Electrochemical Science*, 12 (2017) 6404.
30. N. Naderi, M. Hashim, K. Saron and J. Rouhi, *Semiconductor Science and Technology*, 28 (2013) 025011.
31. V. Maurice, H. Peng, L.H. Klein, A. Seyeux, S. Zanna and P. Marcus, *Faraday discussions*, 180 (2015) 151.
32. S. Kakooei, H.M. Akil, A. Dolati and J. Rouhi, *Construction and Building Materials*, 35 (2012) 564.
33. J. Setina, A. Gabrene and I. Juhnevica, *Procedia Engineering*, 57 (2013) 1005.

34. E. Volpi, A. Olietti, M. Stefanoni and S.P. Trasatti, *Journal of Electroanalytical Chemistry*, 736 (2015) 38.
35. C. Wang, S. Yang, Y. Chen, B. Wang, J. He and C. Tang, *RSC Advances*, 5 (2015) 34580.